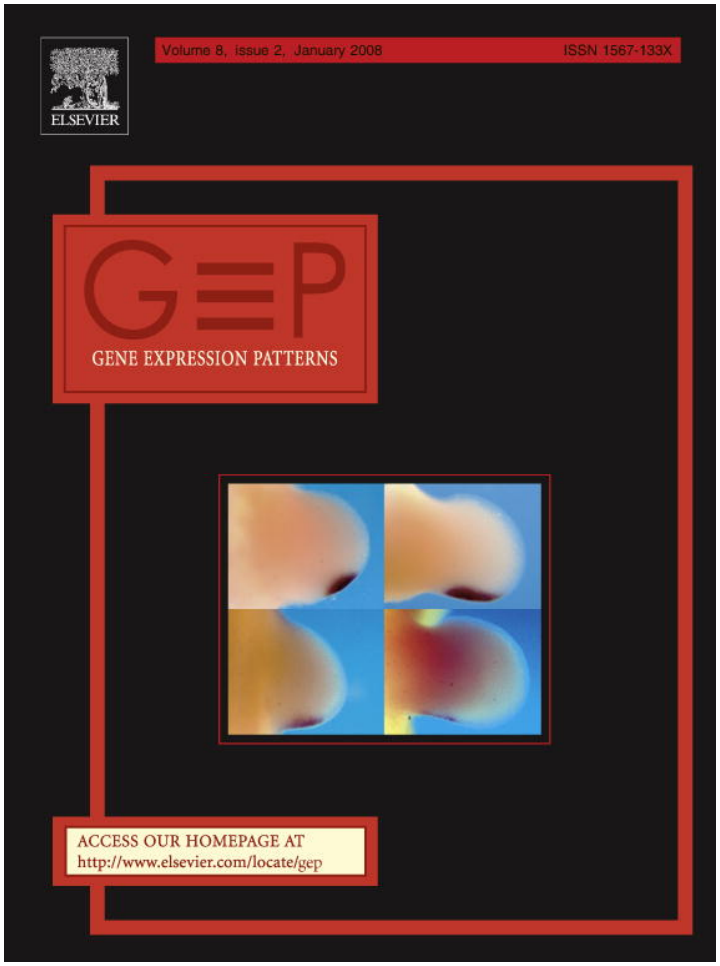

ELSEVIER

Gene Expression Patterns 8 (2008) 124–139

GEP

www.elsevier.com/locate/gep

Characterization of the mid-foregut transcriptome identifies genes regulated during lung bud induction

Guetchyn Millien [a], Jennifer Beane [a,d], Marc Lenburg [c], Po-Nien Tsao [a], Jining Lu [a], Avrum Spira [a,b,d], Maria I. Ramirez [a,b,*]

[a] *Pulmonary Center, Department of Medicine, Boston University School of Medicine, Evans Biomedical Research Center, 650 Albany Street, X-440, Boston, MA 02118, USA*

[b] *Department of Pathology, Laboratory Medicine, Boston University School of Medicine, Boston, MA 02118, USA*

[c] *Department of Genetics and Genomics, Boston University School of Medicine, Boston, MA 02118, USA*

[d] *Bioinformatics Program, Boston University College of Engineering, Boston, MA 02118, USA*

Received 30 October 2006; received in revised form 31 August 2007; accepted 14 September 2007
Available online 26 September 2007

Abstract

To identify genes expressed during initiation of lung organogenesis, we generated transcriptional profiles of the prospective lung region of the mouse foregut (mid-foregut) microdissected from embryos at three developmental stages between embryonic day 8.5 (E8.5) and E9.5. This period spans from lung specification of foregut cells to the emergence of the primary lung buds. We identified a number of known and novel genes that are temporally regulated as the lung bud forms. Genes that regulate transcription, including DNA binding factors, co-factors, and chromatin remodeling genes, are the main functional groups that change during lung bud formation. Members of key developmental transcription and growth factor families, not previously described to participate in lung organogenesis, are expressed in the mid-foregut during lung bud induction. These studies also show early expression in the mid-foregut of genes that participate in later stages of lung development. This characterization of the mid-foregut transcriptome provides new insights into molecular events leading to lung organogenesis.

Keywords: Lung; Development; Organogenesis; Foregut; Endoderm; Embryo; Mouse; Microarray; RNA amplification; Gene expression; Real-time PCR; Laser capture microdissection; Transcription factors; Chromatin remodeling; Fox; Notch; Isl1

Between E7.5 and E9.5 of mouse development, remarkable morphogenetic changes take place in the ventral foregut resulting in formation of distinct organs including pancreas, liver, thyroid, and lung (Grapin-Botton and Melton, 2000; Wells and Melton, 1999). Organ-specific genes such as Pdx1 (pancreas) (Murtaugh and Melton, 2003), albumin (liver) (Jung et al., 1999), Hhex and Pax8 (thyroid) (Parlato et al., 2004) and thyroid transcription factor 1 (thyroid and lung) (DeFelice et al., 2003; Desai et al., 2004; Kimura et al., 1999) demarcate different regions of the foregut as development progresses. By E9 of development, embryos containing between 16 and 20 somites already show thyroid, liver and pancreas primordia but the mid-foregut region, between the pharyngeal arches and the liver and pancreas buds, is still a tube that shows no sign of lung bud formation. In this environment, the trachea and the lung evaginate from the ventral and ventrolateral foregut respectively at approximately E9.5 (Cardoso and Lu, 2006; Warburton et al., 2005). These developmental events are regulated by fibroblast growth factors, bone morphogenetic proteins, retinoic acid, and sonic hedgehog, and their receptors among other factors (Bellusci et al., 1997; Desai et al., 2004; Jung et al., 1999; Litingtung et al., 1998; Rossi et al., 2001; Sakiyama

* Corresponding author. Address: Pulmonary Center, Department of Medicine, Boston University School of Medicine, Evans Biomedical Research Center, 650 Albany Street, X-440, Boston, MA 02118, USA. Fax: +1 617 638 7530.
E-mail address: mramirez@bu.edu (M.I. Ramirez).

1567-133X/$ - see front matter © 2007 Elsevier B.V. All rights reserved.
doi:10.1016/j.modgep.2007.09.003

et al., 2003; Sekine et al., 1999; Warburton et al., 2005; Weaver et al., 2000). These signaling networks activate downstream effectors in both foregut mesoderm and endoderm to induce organ specific gene expression (Cleaver and Krieg, 2001; Horb, 2000; Jung et al., 1999; Kumar et al., 2003; Matsumoto et al., 2001; Wells and Melton, 2000).

Compared to the detailed understanding of the programs leading to formation of the liver and pancreas (Bort et al., 2006; Lee et al., 2005; Lemaigre and Zaret, 2004; Murtaugh and Melton, 2003; Serls et al., 2005; Tremblay and Zaret, 2005), the lung morphogenetic program has not been explored in detail, in large part due to the paucity of marker molecules known to be expressed in the presumptive lung region of the foregut. Microarray studies have been used to characterize profiles of gene expression in embryonic tissues including preimplantation mouse embryos (Sherwood et al., 2007; Zeng et al., 2004), prepancreas, and early pancreatic endodermal cells (Gu et al., 2004). The latter database has been particularly important for the identification of genes involved in acquisition of pancreatic cell fate and has also established the transcriptional profiles of endodermal precursors. To date, global profiles of gene expression in the developing lung have been focused on the processes of branching morphogenesis and on perinatal lung development (Banerjee et al., 2004; Bonner et al., 2003; Lu et al., 2005, 2004a), but there are not yet similar data on molecular changes that accompany the initiation of lung organogenesis.

We report herein the characterization of the transcriptome of the lung region of the foregut (referred as mid-foregut) prior and during initiation of lung organogenesis, including trachea and primary bud formation. We have identified genes expressed in mid-foregut cells, and genes whose expression levels change during lung primordium formation.

1. Results and discussion

1.1. Developmental lung genes are expressed in the prospective lung region of the foregut

We studied temporal differences in gene expression in mid-foregut tissues containing endoderm and mesoderm cells isolated by microdissection at three developmental stages prior and after lung bud formation (16–20, 21–25, and 26–30 somite stages) (Fig. 1a and b). We determined by real-time RT-PCR (QRT-PCR) whether the tissues to be used in the microarray studies expressed lung and liver marker genes. Twenty-four hours before lung budding, at E8.5, the mid-foregut already expresses lung developmental genes. Thyroid transcription factor 1 (Titf-1, TTF-1, Nkx2.1), a transcription factor critical for lung cell differentiation (Kimura et al., 1999), was detected in the mid-foregut tissue at all three developmental stages, and the level of expression was increased as the primary lung buds formed (Fig. 1c); although Titf-1 is also expressed during thyroid organogenesis, the thyroid was excluded from the mid-foregut samples analyzed, as shown in Fig. 1a and b. Fibroblast growth factor 10 (FGF10) expressed in the foregut mesenchyme can be detected at the three developmental stages, and significantly increases in 26–30 somite vs. 21–25 somite foreguts (Fig. 1c). Surfactant protein C (SP-C) mRNA, a lung-specific gene (Khoor et al., 1994; Wang et al., 1994), expressed very early in lung development and a downstream target of Titf-1, was not detected in 16–20, 21–25, or 26–30 somite embryos by QRT-PCR (data not shown) but can be detected later in the mid-foregut endoderm of embryos containing more than 30 somites (Fig. S1A and B, supplementary material). Albumin mRNA was not detected in the mid-foregut by real-time PCR (data not shown), but is highly detected in the posterior foregut endoderm (liver), isolated by laser capture microdissection from embryos containing more than 30 somites (Fig. S1A and B, supplementary material). Microarray analyses of amplified mid-foregut RNA show expression of the lung expressed genes T1α and caveolin-1 (Ramirez et al., 2002; Williams et al., 1996), and marked reduction of the liver genes α-fetoprotein and transthyretin (Jung et al., 1999; Lee et al., 2005), as development proceeds (Table S3, supplementary material). Pax8, a thyroid gene expressed also in the branchial arches (Trueba et al., 2005) was detected at low levels in the 16–20 somite samples, and its level remains low and unchanged during lung bud formation (Table S3, supplementary material). Overall, these data confirm the specific nature of the regions selected to study. The exact timing of lung cell specification in the multipotent foregut has not been clearly determined, but detection of Titf-1 and FGF10 in the mid-foregut at E8.5 indicates certain commitment of the cells to start lung formation (Desai et al., 2004).

1.2. Statistical analysis and functional classification of the microarray data

Three independent mRNA samples, at each of the developmental stages selected (16–20s, 21–25s, and 26–30s), were amplified and analyzed by microarrays (total of nine arrays). Hierarchical clustering analysis of genes significantly up-regulated or down regulated across all nine samples, with ANOVA and Student's *t*-tests $p \leqslant 0.05$ and detection $p \leqslant 0.05$ are shown in Fig. 2a and b. The result illustrates that the general premise of this study is correct, i.e. that significant changes in gene expression accompany the induction of the lung as it emerges from the foregut at the 26–30 somite stage.

A number of comparisons are possible to analyze the data. We chose to identify differences between early and late foreguts as representing the absence and the presence of lung buds. Relative to the earliest group, 104 genes are up-regulated more than 1.8-fold and 119 genes down-regulated more than 1.8-fold in the late group undergoing lung organogenesis. Although a change higher than 2-fold has been conventionally used to consider genes as functionally important, we have opted to use 1.8-fold as cut-off level

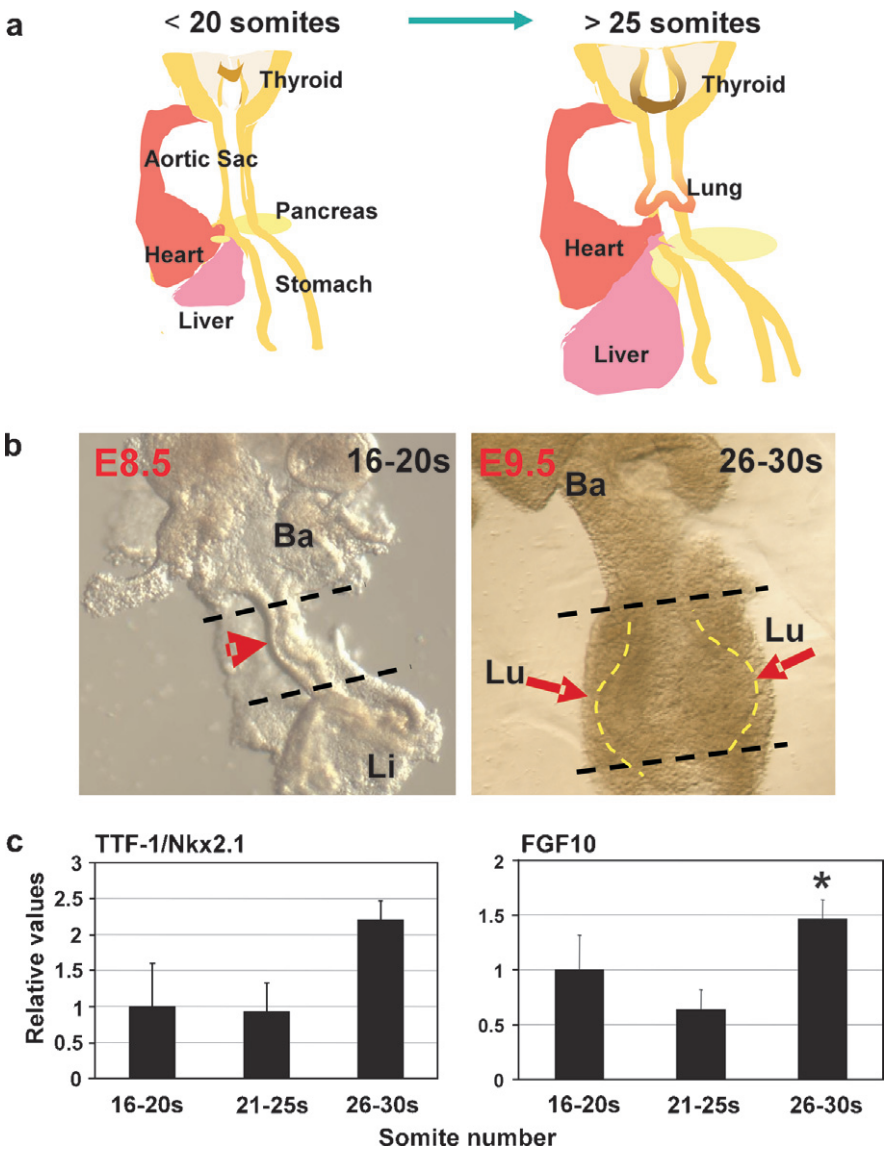

Fig. 1. Mid-foregut tissue was isolated to study gene expression profiles at three developmental stages. (a) Graphic representation of the morphology of the foregut in embryos containing 11–25 somites (E8.0–E9.5), and in embryos containing more than 25 somites (E9.5–10). Endoderm derived organs (thyroid, pancreas, liver, and lung) are depicted. The relative position of those organs to the cardiac mesoderm is represented. (b) Microscopic appearances of partially dissected mid-foreguts from 16 to 20 somite embryos (E8.5) (red arrowhead), and from 26 to 30 somite embryos (E9.5). The mid-foregut tissue between the black dashed lines was collected for further analyses. The earliest samples (16–20 somites) show evidence of primitive thyroid and liver/pancreas budding at the extremes of the mid-foregut field from which the lung is derived. Embryos with greater than 25 somites have initiated formation of bilateral lung buds (outlined in yellow). Ba, branchial arches; Li, liver; Lu, lung buds, outlined by yellow dashed lines. (c) TTF-1 (Nkx2.1, Titf1) and FGF10 mRNA levels, assessed by real-time RT-PCR, in mid-foreguts dissected from 16 to 20, 21 to 25, and 26 to 30 somite mid-foreguts. Titf-1 and FGF10 mRNA levels are normalized to GAPDH. Data are expressed relative to 16–20 somite mid-foregut samples. $n = 3$ Error bars represent standard error of the mean. *Indicates t test $\leqslant 0.05$.

due to the high number of genes showing a statistically significant change between 1.8- and 2-fold. A number of previous studies also opted to use lower cut-off levels (1.2–1.5) when the changes are highly significant (Jeong et al., 2005; Lu et al., 2004b; McReynolds et al., 2005). Enriched biological themes within the up-regulated genes and the down-regulated genes were identified using appropriate computer algorithms (Fig. 2c and d). The most significantly overrepresented, up-regulated biological process (ease score $= 3.35 \times 10^{-3}$) was regulation of transcription (Fig. 2c). That group contains largely, but not solely, transcription factors; many have not been previously shown to be related to lung development. Some of these transcription factors were further analyzed by QRT-PCR and whole mount in situ hybridization. Within the down-regulated genes, macromolecule/protein biosynthesis was the most significantly overrepresented biological process (ease score $= 3.23 \times 10^{-9}$) (Fig. 2d). Some transcriptional regulatory genes were also down-regulated. Genes categorized as functioning in proliferation, transport, and organization and biogenesis are represented in both the up- and down-regulated groups.

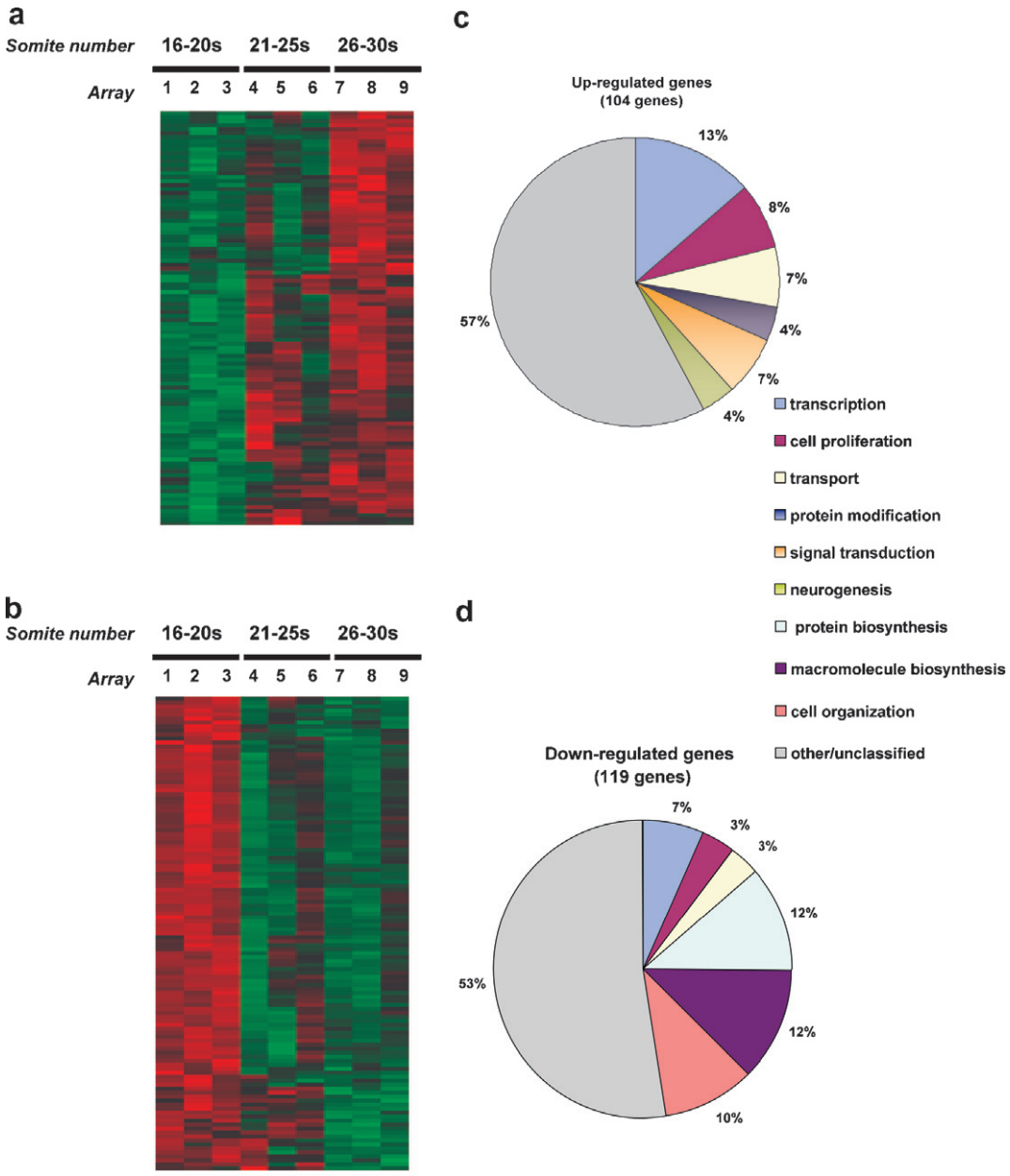

Fig. 2. Cluster graphs of (a) genes up-regulated $\geqslant 1.8$-fold, and (b) genes down regulated $\geqslant -1.8$-fold from 16 to 20 somite to 26–30 somite embryos (detection $p \leqslant 0.05$, ANOVA $p \leqslant 0.05$, and Student's t test $p \leqslant 0.05$). Green color indicates low expression, red indicates high expression. Three independent arrays were analyzed for each developmental stage (arrays 1–3, 16–20 somite mid-foregut samples; arrays 4–6, 21–25 somite mid-foregut samples; arrays 7–9, 26–30 somite mid-foregut samples). (c) Pie chart showing the GO classification of the functional groups of the 104 genes up-regulated shown in (a). (d) Pie chart showing the GO classification of the functional groups of the 119 genes down-regulated shown in (b).

To find genes enriched in each of the three time points studied, especially in the intermediate time point (21–25 somite stage), a parametric ANOVA was performed. One-thousand seventy-six probe sets with a p-value less than 0.05 were selected for further analysis by K-means clustering (Fig. 3). Five clusters (a–e) were generated in which genes decline from 16–20 to 21–25 somites or to 26–30 somites, increase from the 16–20 somite stage with a peak at 26–30 somites, or peak in the middle at the 21–25 stage, or increase from 21–25 to 26–30 somites. We listed in Table 1 genes that are enriched in each developmental time point identified by ANOVA and/or Student's t tests, and are involved in transcriptional regulation. These genes include factors that bind directly to cis-elements in the DNA, co-factors, and genes that form chromatin modifying complexes. For a complete list of genes see Tables S4–S6 in supplementary material.

1.3. Real-time RT-PCR confirmation of temporal changes in gene expression

Forty-three genes shown to change level of expression during lung induction were analyzed by QRT-PCR using non-amplified mid-foregut RNA. mRNA levels in 26–30

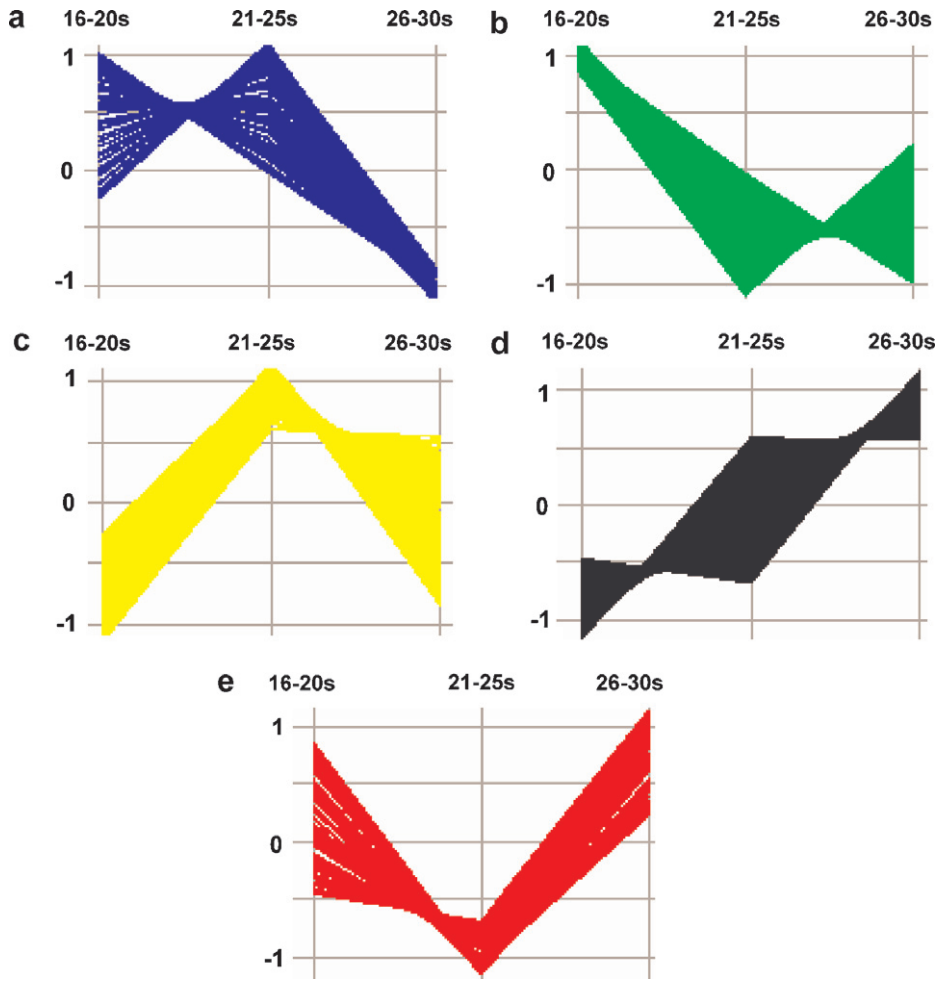

Fig. 3. Patterns of gene expression identified by K-means clustering analysis of genes that pass the ANOVA test comparing the three developmental points studied 16–20, 21–25, and 26–30 somite embryos (ANOVA $p \leqslant 0.05$). (a) Genes that are down-regulated from 16–20 to 26–30 somites; (b) genes that are down-regulated from 16–20 to 21–25 somites; (c) genes that peak at 21–25 somites; (d) genes that are up-regulated from 16–20 to 26–30 somites; (e) genes that are up-regulated from 21–25 to 26–30 somites. The complete list of genes is in the supplemental material. Axes: x, developmental stage; y, z-score normalized values, 0, mean of the average for each gene; ± 1, standard deviation.

somite samples normalized to GAPDH mRNA levels were expressed relative to the 16–20 somite samples set at a relative value of one. A similar semi-quantitative comparison of the same genes was done for the microarray data. As shown in Fig. 4a and b and Fig. S3A and B, 19 out of 43 genes tested showed statistically significant changes in expression by QRT-PCR correlating well to the microarray data, although the absolute fold-differences do not match precisely as would be expected due the different nature of the methods and the analysis of different samples. In addition, the trend in expression patterns of other 12 genes (e.g. Cbfa2t1, Cbx4, Six1) was confirmed by QRT-PCR, although the fold change observed by this method was not statistically significant ($p > 0.05$) (Table S7A). The remaining 12 genes tested did not match the microarray data (Table S7B).

1.4. Transcription factors and co-factors are developmentally regulated as the lung buds form

The largest change demonstrated by QRT-PCR analysis is in the LIM domain transcription factor Isl1 (Thor et al., 1991). Isl1 is necessary for proliferation and survival of cells in the foregut mesoderm and dorsal pancreatic mesenchyme, and is linked to cell fate decision in motor neurons (Pfaff et al., 1996), cardiac cells (Cai et al., 2003), and pancreatic islets (Ahlgren et al., 1997) but has not been previously implicated in lung development. Isl1 null mice [Isl1(−/−)] are developmentally arrested soon after E9.5, show abnormal organization of the vascular endothelium, and severely abnormal heart development with reduction of the amount of atrial tissue. Expression of FGF10, Bmp4, and Bmp7 is highly down-regulated in pharyngeal endoderm and splanchnic mesoderm in the absence of Isl1 at E8.5–9.0, likely as a result of direct or indirect regulation of these growth factors by Isl1 and/or viability of the foregut cells. A recent publication indicates a putative cis-element for Isl1 in the FGF10 promoter (Ohuchi et al., 2005). We now show that Isl1 is transiently expressed in the early stages of lung morphogenesis and its expression is down regulated as the lung begins branching morphogenesis. Early lethality of the Isl1 null mutation precludes to study the role of Isl1 in lung budding.

Table 1
Genes involved in transcription differentially regulated as the lung buds form

Gene	Affymetrix ID	Fold change			
		16–20s	21–25s	26–30s	Stat
Genes enriched at 16–20s					
Transcription factors					
Nfia	1421163_a_at	1.0	−1.5	−3.2	*t*
Ehox	1419229_at	1.0	−1.6	−2.9	*a*
Sp7	1418425_at	1.0	−1.1	−2.3	*a*, *t*
Twist 1	1418733_at	1.0	1.3	−2.0	*a*, *t*
Zfp52	1426471_at	1.0	−1.7	−1.9	*a*
Fhl2	1419184_a_at	1.0	−1.2	−1.9	*a*, *t*
Hoxa1	1420565_at	1.0	−1.5	−1.7	*a*
Cebpg	1451639_at	1.0	−1.6	−1.6	*a*
Rfx3	1425413_at	1.0	1.0	−1.6	*a*
Mesp1	1426557_at	1.0	1.1	−1.5	*a*
Esrrg	1421747_at	1.0	−1.7	−1.5	*a*
Runx2	1425389_a_at	1.0	−1.6	−1.4	*a*
Gtf2h4	1417093_a_at	1.0	−1.7	−1.4	*a*
Co-factors					
Scand1	1448868_at	1.0	−3.0	−2.8	*t*
Lsm4	1448622_at	1.0	−1.9	−2.7	*a*, *t*
Six1	1427277_at	1.0	−1.3	−2.6	*a*
Fabp1	1417556_at	1.0	−2.9	−1.9	*a*
Hsbp1	1451162_at	1.0	−1.8	−1.9	*a*
Med8	1431423_a_at	1.0	−1.9	−1.8	*a*
Pdlim1	1416554_at	1.0	−1.8	−1.8	*a*
Six3	1427523_at	1.0	1.1	−1.6	*a*
Piasy	1418861_at	1.0	−1.3	−1.5	*a*
Hcngp	1449295_at	1.0	−2.0	−1.5	*a*
Thap7	1452069_a_at	1.0	−1.6	−1.4	*a*
Snapc2	1436703 x_at	1.0	−1.5	−1.2	*a*
Sertad3	1421076_at	1.0	−1.6	−1.2	*a*, *t*
Chromatin remodeling factors					
Sap18	1419444_at	1.0	−1.7	−2.2	*a*, *t*
Hmgn3	1431777_a_at	1.0	−1.4	−1.9	*a*
Chrac1	1422505_at	1.0	−1.6	−1.6	*a*, *t*
Ruvbl1	1416585_at	1.0	−1.6	−1.2	*a*
Sin3b	1424355_a_at	1.0	−1.5	−1.1	*a*
Genes enriched at 21–25s					
Transcription factors					
Nf1b	1438245_at	1.0	4.8	2.3	*t*
Zbtb1	1424750_at	1.0	2.7	2.3	*a*, *t*
Atf2	1426582_at	1.0	2.6	1.9	*a*, *t*
Rfx5	1423103_at	1.0	2.6	1.9	*a*
Nr3c1	1460303_at	1.0	2.6	2.4	*a*
Mafk	1418616_at	1.0	2.3	1.4	*a*
Foxm1	1448833_at	1.0	1.7	1.3	*t*
Meox1	1417595_at	1.0	1.5	−1.4	*a*
E2f6	1448835_at	1.0	1.5	1.3	*a*
Srf	1418255_s_at	1.0	1.5	1.2	*a*
Gabpb1	1436232_a_at	1.0	1.5	1.2	*a*
Irx5	1421072_at	1.0	1.5	−1.2	*a*
Co-factors					
Dnajc1	1420500_at	1.0	3.9	2.0	*a*
Zmynd11	1426531_at	1.0	2.0	1.3	*a*
Phr1	1434937_at	1.0	1.6	−1.1	*a*
Ncor1	1423200_at	1.0	1.6	1.1	*a*
Chromatin remodeling factors					
Ezh1	1449023_a_at	1.0	1.8	1.4	*a*
Hp1bp3	1415751_at	1.0	1.7	1.5	*a*
d2	1417165_at	1.6	1.0	1.5	*a*, *t*
Ncoa1	1434515_at	1.0	1.5	1.4	*a*, *t*
Genes enriched at 26–30s					
Transcription factors					
Bcl11a	1419406_a_at	1.0	2.3	5.6	*a*, *t*
Six5	1427560_at	1.0	4.3	4.3	*a*, *t*
Hoxa4	1427354_at	1.0	1.9	4.1	*a*, *t*
Ets1	1452163_at	1.0	1.9	3.1	*a*, *t*
Foxp1	1435222_at	1.0	1.0	3.0	*a*, *t*
Msc	1418417_at	1.0	1.4	2.8	*a*, *t*
Hoxa5	1448926_at	1.0	1.4	2.5	*t*
Elf1	1417540_at	1.0	2.0	2.3	*t*
Hoxb8	1452493_s_at	1.0	1.5	2.3	*a*, *t*
Zfp71-rs1	1424752_x_at	1.0	1.8	2.3	*t*
Id4	1450928_at	1.0	1.7	2.2	*a*
Isl1	1450723_at	1.0	1.3	2.1	*a*, *t*
Pitx2	1424797_a_at	1.0	1.3	2.1	*a*, *t*
Sp4	1437508_at	1.0	2.0	2.1	*t*
Foxf2	1418220_at	1.0	1.9	2.0	*t*
Zfp37	1419207_at	1.0	1.2	2.0	*a*
Rb1	1417850_at	1.0	1.4	2.0	*t*
Tcf4	1434148_at	1.0	1.7	1.9	*a*
Tcfap4	1418167_at	1.0	1.1	1.9	*t*
Zfp26	1427120_at	1.0	1.4	1.7	*a*
Co-factors					
Rbbp4	1454791_a_at	1.0	1.3	3.7	*a*
Zfpm2	1449314_at	1.0	2.6	3.5	*t*
Zfp467	1419564_at	1.0	3.8	3.2	*a*, *t*
Rab2	1419946_s_at	1.0	2.4	3.1	*a*, *t*
Strap	1419913_at	1.0	1.6	2.5	*a*, *t*
Zik1	1433946_at	1.0	1.3	2.4	*a*, *t*
Ilf2	1417948_s_at	1.0	1.5	2.2	*t*
Dach2	1449823_at	1.0	1.5	2.2	*a*, *t*
Khdrbs1	1437389_x_at	1.0	1.9	1.9	*t*
Dr1	1416018_at	1.0	1.7	1.9	*t*
Mcm3	1420029_at	1.0	1.5	1.9	*t*
Hmga2	1422851_at	1.0	1.6	1.8	*a*
Tle1	1422751_at	1.0	1.7	1.7	*a*
Cri1	1448405_a_at	1.0	1.3	1.7	*a*
Btg1	1426083_a_at	1.0	1.1	1.7	*a*
Hmga2	1450780_s_at	1.0	1.5	1.7	*t*
Chromatin remodeling factors					
Suz12	1449661_at	1.0	2.5	2.9	*a*
Ing3	1450760_a_at	1.0	1.6	2.4	*t*
Smcy	1424903_at	1.0	1.0	2.2	*a*
Cbx4	1419583_at	1.0	1.5	2.2	*t*
Bmi1	1448733_at	1.0	1.5	2.1	*a*, *t*
Rnf2	1451519_at	1.0	1.2	2.0	*a*
Smarce1	1422676_at	1.0	1.2	1.9	*t*
Chmp1b	1418817_at	1.0	1.6	1.9	*a*
Carm1	1419743_s_at	1.0	1.3	1.7	*a*, *t*
Dnmt3a	1460324_at	1.0	1.3	1.7	*a*, *t*
Pspc1	1423192_at	1.0	1.3	1.7	*a*

Statistics: *t*, Student's *t* test $p \leqslant 0.05$; *a*, ANOVA $p \leqslant 0.05$.
A Student's *t* test was used to compare the earliest vs. the latest time point (16–20s to 26–30s).
Genes with $p \leqslant 0.05$ are indicated with *t*.
A parametric ANOVA was performed to find genes differentially expressed between two or more of the three groups.
Genes with $p \leqslant 0.05$ are indicated with *a*.
Genes enriched at 16–20s are down regulated as the lung buds.
Genes enriched at 21–26s peak before lung buds.
Genes enriched at 26–30s are up-regulated as the lung buds.
Genes involved in transcription were selected and divided in three functional groups, transcription factors, co-factors, and chromatin remodeling factors.

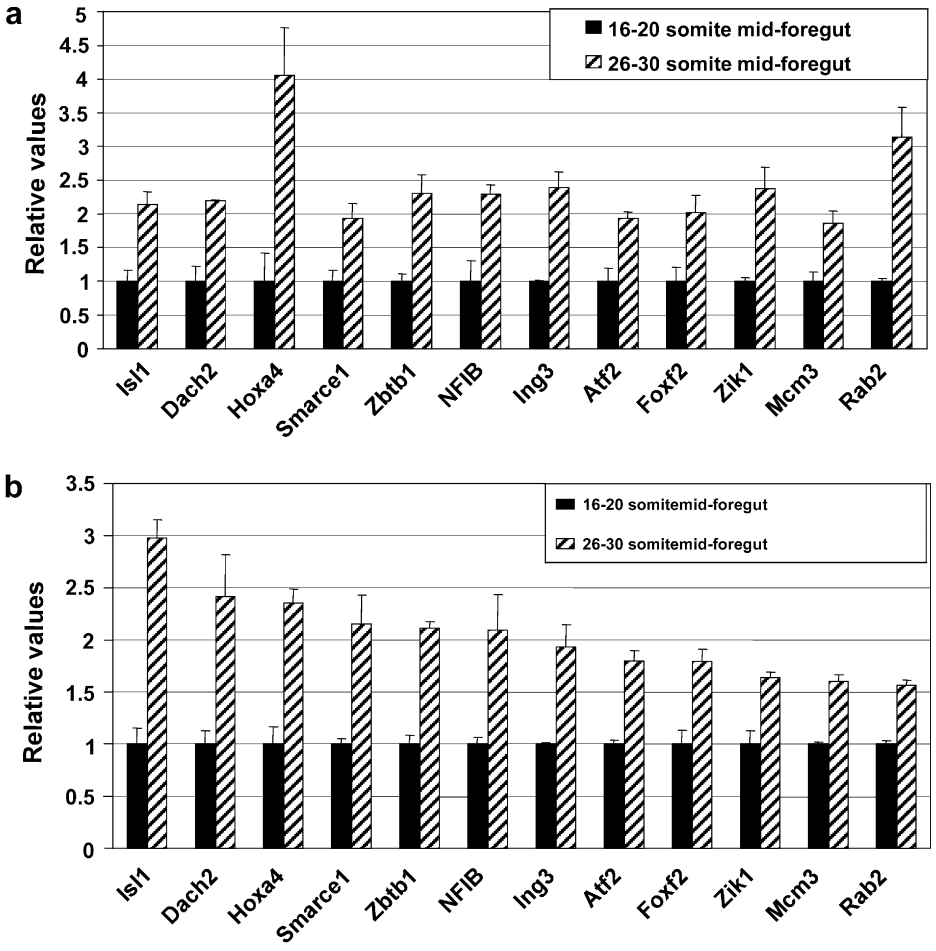

Fig. 4. Real-time RT-PCR validation of selected transcription related genes identified by microarrays. (a) Expression levels obtained in the microarray analysis of amplified RNA from 16 to 20 somite mid-foreguts (relative value = 1, black bars) compared to 26–30 somite mid-foreguts (fold change relative to 16–20 somite samples, hatched bars). (b) Real-time RT-PCR validation of the genes depicted in (a). Non-amplified RNA from 16 to 20 somite mid-foreguts (relative value = 1, black bars) compared to 26–30 somite mid-foreguts (fold change relative to 16–20 somite samples, hatched bars). Data are normalized to GAPDH expression level. $n = 3$. Error bars represent standard error of the mean.

Other transcription factors that directly bind to DNA validated by QRT-PCR include HoxA4 (Packer et al., 2000), NFIB (Chaudhry et al., 1997), and Foxf2 (Aitola et al., 2000). We have identified by microarrays expression in the mid-foregut region of other Fox genes that were not previously linked to the process of lung bud formation. Most of the Fox genes were detected at high levels and did not change over the time period studied. Fox transcription factors play important roles in development (Lee et al., 2005), and during induction of the endoderm derived organs (Carlsson and Mahlapuu, 2002). Foxa2 and Foxa1 are critical for initial steps in foregut tube closing and viability of endodermal cells (Ang and Rossant, 1994). They also regulate expression of several lung genes including surfactant protein genes (Costa et al., 2001). Other Fox factors, such as Foxf1, Foxp1, and Foxb1, are regulators of later events in lung development (Costa et al., 2001).

Changes in level of expression of the Dach2 co-factor, that belongs to the Eya/Six/Dach transcriptional complex involved in cell fate decisions in other organs (Davis et al., 2001), was validated by QRT-PCR. Three members of these complexes, sine-oculis 1 (Six1) and −5 (Six5) and Daschund 2 (Dach2) change their level of expression as the lung buds; Six1 is down regulated, and Six5 and Dach 2 are up-regulated. Eya/Six/Dach complexes can switch between gene activation and repression of gene expression depending on the members of the family that form these complexes.

Four additional genes showing a large increase in 26–30 somite samples compared to 16–20 somite samples in the microarray analysis were measured by QRT-PCR of non-amplified mRNA and confirmed the original findings (Fig. S3A and B, supplementary material). The putative functions of these molecules are diverse and include the enzymes α-2,8-sialyltransferase 8A (Yoshida et al., 1995) and 3-oxoacid CoA transferase 1 (Ganapathi et al., 1987), the apoptosis-related gene caspase 7 (Lakhani et al., 2006), and syndecan 2 (David et al., 1993) among others.

1.5. Expression of selected transcription factor and signaling gene families during lung bud formation

We evaluated microarray data for expression of members of the Fox, Hox, Tbx, GATA transcription factor families (Table 2) and genes of selected signaling pathways that participate in lung development including FGFs, Bmps, Shh, Retinoic Acid, and Notch pathways (Table 3) (Cardoso, 1995; Cardoso and Lu, 2006; Warburton et al., 2005). We have detected Foxa1, Foxa2, Hox A4, A5, B4, B5, B8; Tbx 1, 2; GATA 5, 6; FGF7, FGF1, FGFRII and IV; Bmp4, and BmpR1a; Notch1 and Dll3 mRNAs among others. QRT-PCR confirmed that HoxA4 and Foxf2 (Fig. 4a and b) are significantly increased in 26–30 somite samples. We anticipated finding expression of FGF10 and Titf-1 (Nkx2.1) but these factors were not detected in the microarray analysis, possibly because they are of very low abundance, are poorly amplified prior to hybridization, and/or the oligos on the microarray are 5′ to the amplified message region as the amplification method is 3′bias (Table S1); however these mRNAs can be readily detected by QRT-PCR in non-amplified mid-foregut samples (Fig. 1C). Microarray analysis of amplified or non-amplified samples can always produce false positive or negative results. Therefore, validation by other methods is necessary. In this study we have analyzed selected genes by QRT-PCR and whole mount in situ hybridization.

Table 2
Selected families of transcription factors detected in the mid-foregut

Gene	Affymetrix ID	Average signal			
		16–20s	21–25s	26–30s	Stat
Fox family					
Foxa1	1418496_at	2093	2252	2844	
Foxa2	1422833_at	635	497	712	
Foxc1	1419486_at	411	565	503	
Foxd1	1418876_at	355	471	460	
Foxf2	1418220_at	56	109	113	*t*
Foxg1	1418357_at	193	331	394	
Foxj2	1420374_at	166	130	174	
Foxk2	1428354_at	374	857	527	
Foxm1	1448833_at	374	639	473	*t*
Foxm1	1417748_x_	231	235	253	
Foxo1	1416983_s_	349	561	540	
Foxp1	1421141_a_	98	81	139	
Foxp1	1421142_s_	218	183	301	
Foxp1	1421140_a_	120	205	131	
Foxp1	1435222_at	522	556	1545	*a*, *t*
Foxp1	1435221_at	1733	2116	2561	*a*, *t*
Foxp3	1455805_x_	341	340	363	
Tbx family					
Tbx1	1425779_a_	391	373	251	
Tbx2	1422545_at	177	232	278	
Tbx3	1448029_at	491	564	503	
Tbx6	1449868_at	84	100	76	
Tbx20	1425158_at	96	101	83	
Gata family					
Gata1	1449232_at	164	106	175	
Gata2	1450333_a_	477	577	510	
Gata4	1418863_at	288	323	330	
Gata5	1450125_at	149	147	172	
Gata5	1450126_at	452	444	448	
Gata6	1425463_at	101	99	89	
Gata6	1425464_at	548	580	498	
Hox family					
Hoxa1	1420565_at	4171	2838	2510	*a*
Hoxa2	1419602_at	188	256	224	
Hoxa3	1427433_s_	100	175	149	
Hoxa4	1427354_at	42	80	172	*a*,*t*
Hoxa4	1420227_at	90	85	125	
Hoxa5	1448926_at	103	149	259	*t*
Hoxb1	1453501_at	539	809	493	
Hoxb2	1449397_at	799	928	801	
Hoxb4	1460379_at	395	408	364	
Hoxb5	1418415_at	421	512	517	
Hoxb7/b8	1452493_s_	81	120	186	*a*
Hoxc4	1422870_at	351	620	608	

t, Student's *t* test $p \leqslant 0.05$.
a, ANOVA $p \leqslant 0.05$.
The table includes the average signal for genes detected in the mid-foregut and lung regions (detection $p \leqslant 0.05$) at 16–20s, 21–25s and 26–30s developmental stages. Only genes with a signal $\geqslant 100$ at any stage are listed. Most genes do not change the level of expression as the lung buds. A few of them change the level of expression significantly indicated by Student's *t* and/or ANOVA tests.

The representation of members of the Fox family is notable as shown in Table 2. Of the 26 Fox family members represented on the microarrays used in the study, 12 are present in the mid-foregut (detection *p* value $\leqslant 0.05$). Foxa1 and Foxa2 display the highest detection levels. However, with the exception of Foxp1 (Shu et al., 2001), Foxm1 (Kim et al., 2005), and Foxf2 (Wang et al., 2003) as shown in Tables 1 and 2, mRNA expression levels of other Fox genes do not change significantly during initiation of the lung budding. Among the signaling pathways, it is notable the number of Notch pathway related genes present in the mid-foregut as the lung forms (24 present in the mid-foregut out off 114 probe sets, Table 3). Changes in Notch 1 (Taichman et al., 2002), Delta-like 3 (Ladi et al., 2005), and presenilin enhancer 2 (Francis et al., 2002) are statistical significant. As the Notch pathway has been shown to regulate early cell fate decisions in other tissues (Louvi and Artavanis-Tsakonas, 2006), its role in lung induction will entail further evaluation.

1.6. Chromatin remodeling and DNA methylation genes change their level of expression during initiation of lung organogenesis

Among several chromatin remodeling genes identified in Table 1, smarce1/BAF57 and Ing3 were confirmed to increase their level of expression significantly as the lung buds. Smarce1/BAF57 is one of the genes that form part of the ATP-dependent chromatin remodeling SWI/SNF complex (Chen and Archer, 2005; Domingos et al., 2002) which modify nucleosomes changing the accessibility of transcription factors to their binding sites on the DNA (Sudarsanam and Winston, 2000). Ing3 is a component of the NuA4 histone acetyltransferase (HAT) complex (Doyon et al., 2004). These proteins are generally linked to gene activation.

Table 3
Selected signaling pathways detected in the mid-foregut

Gene	Affymetrix ID	Average signal			
		16–20s	21–25s	26–30s	Stat
FGF pathway					
FGF1	1450869_at	160	169	98	*t*
FGF7	1422243_at	111	113	116	
FGF 13	1418497_at	570	664	743	
FGFRII	1420847_a_	164	155	155	
FGFRIII	1421841_at	375	399	441	
FGFRV	1451912_a_	144	248	190	
FGFRap1	1424615_at	346	321	427	
Bmp pathway					
Bmp1	1426238_at	347	355	407	
Bmp4	1422912_at	304	337	434	
Bmp 7	1435479_at	361	413	452	
BmpR1a	1425491_at	248	266	296	
BmpR1a	1425492_at	2055	3039	2974	
BmpR1a	1425493_at	307	530	473	
BmpR1a	1425494_s_	535	1009	780	
BmpR1a	1451729_at	426	421	326	
Smad1	1448208_at	815	1251	1215	
Smad5	1451873_a_	189	279	233	
Grem1	1425357_a_	147	125	80	*a,t*
Bambi	1423753_at	901	674	548	
Bmp2k	1437419_at	111	169	290	
Shh/Ptch pathway					
Ptch	1428853_at	5813	7243	7193	
Smo	1427049_s_	2197	2318	2453	
Smo	1427048_at	346	309	443	
Gli1	1449058_at	163	179	205	
Gli2	145921 1_at	1465	1913	1929	
Gli2	1446086_s_	139	197	150	
Hhip	1421426_at	124	95	197	*a*
Hhip	1438083_at	41	63	111	*a,t*
Zic1	1423477_at	60	113	48	
Retinoic acid pathway					
Crabp1	1448326_a_	1329	508	338	
Crabp2	1451191_at	881	543	481	*t*
Rai1	1453200_at	255	416	315	
Rai12	1431411_a_	1496	1135	993	
Stra13	1433574_at	141	115	147	
Raet1a	1420603_s_	532	300	295	
Notch pathway					
Notch1	1418634_at	185	480	203	*a*
Notch2	1455556_at	896	876	603	
Notch3	1421965_s_	1069	1151	1069	
Dll1	1419204_at	179	275	252	
Dll3	1449236_at	100	204	250	*t*
Dtx2	1439429_x_	1956	1833	1867	
Dtx3	1420752_at	229	258	289	
Psen1	1421853_at	1064	1161	1079	
Psenen	1415679_at	2563	1924	1299	*a*
Rbpsuh	1448957_at	402	691	719	
Maml1	1426769_s_	931	1438	1253	
Mib1	1451818_at	278	267	235	
Mib2	1424862_s_	202	193	160	
Sbno1	1426559_at	135	334	143	
Sbno1	1434612_s_	276	417	359	
Sbno1	1451436_at	186	255	258	
App	1420621_a_	184	212	180	
App	1427442_a_	3160	4941	3498	
Aph1a	1424979_at	217	216	217	
Aph1a	1424980_s_	569	378	547	
Aph1a	1451554_a_	238	216	192	*a*
Fbxw7	1451558_at	499	426	539	
Il6st	1452843_at	348	521	325	
Nrarp	1417985_at	395	527	512	
Trp63	1418158_at	130	141	125	
Wdr12	1448646_at	729	735	501	

t, Student's *t* test $p \leqslant 0.05$.
a = ANOVA $p \leqslant 0.05$.
The table includes the average signal for genes detected in the mid-foregut and lung regions (detection $p \leqslant 0.05$) at 16–20s, 21–25s and 26–30s developmental stages. Only genes with a signal $\geqslant 100$ at any stage are listed. Most genes do not change the level of expression as the lung buds. A few of them change the level of expression significantly indicated by Student's *t* and/or ANOVA tests.

Some polycomb family genes (PcG) such as Suz12, Cbx4, and Rnf2 (Ringrose and Paro, 2004) and the DNA methylation genes Dnmt3a and Mbd2 (Li, 2002) linked to gene silencing are up-regulated in the mid-foregut region as the lung bud forms. Many of these genes are ubiquitously expressed but an increase in the level of expression during lung induction highlights the importance of chromatin remodeling and DNA methylation in lung organogenesis (Lee et al., 2006).

1.7. Anterior–posterior patterns of gene expression in the foregut endoderm

The presence of distinct molecular fields within the anterior–posterior axis of the foregut endoderm was shown by QRT-PCR analysis of laser capture microdissected foregut epithelium that is free of adjacent mesenchymal cells (Fig. 5a). This procedure allows the collection of regional epithelial samples representing anterior, mid, and posterior areas of the foregut endoderm. In 21–25 somite samples the patterns of expression of three transcription factors differ along the anterior–posterior foregut axis (Fig. 5b). Irx5, a member of the Iroquois homeobox gene family expressed in the E9.5–10.5 foregut (Cohen et al., 2000), is expressed at similar levels in the three regions. In contrast Hlxb9 mRNA is highly expressed in the most posterior sample with low to marginally detectable levels in the mid and anterior samples. This is consistent with its essential role in specification of gut epithelial cells to a pancreatic fate (Li et al., 1999). FoxO1, a homeobox transcription factor shown to inhibit pancreas-specific genes (Kitamura et al., 2002), is expressed in a linear gradient opposite to that of Hlxb9 with the highest levels anteriorly. In 26–30 somite samples, the patterns of expression of three genes identified in the microarray analysis, Isl1, Dach2, and smarce1/BAF57, also differ along the anterior–posterior foregut axis (Fig. 5c). Isl1 is detected in the mid-and posterior foregut endoderm at similar levels, but higher than in the anterior endoderm. Dach2, is higher in the mid-foregut endoderm than in neighboring regions, while smarce1 is higher in

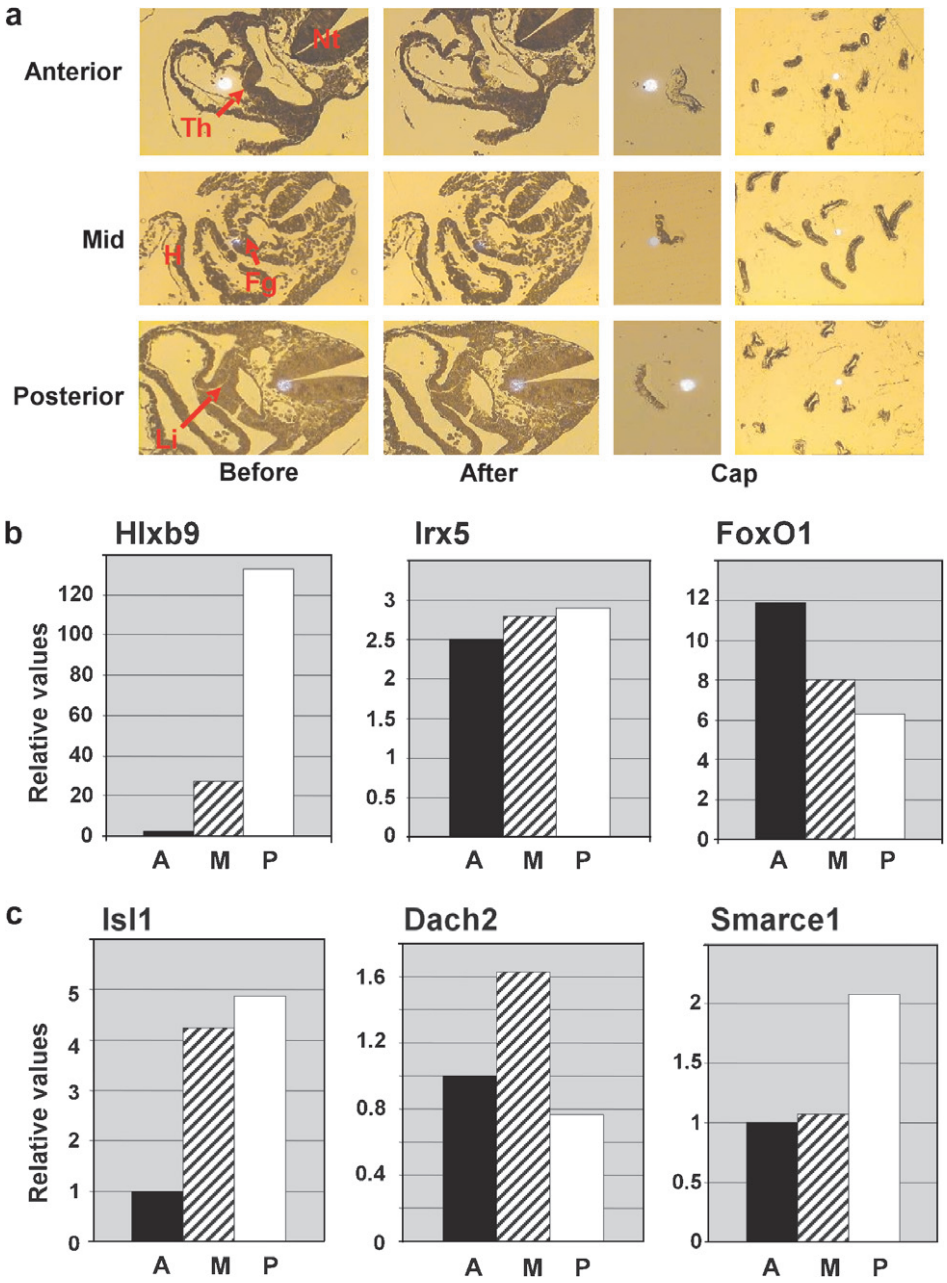

Fig. 5. (a) Representative laser capture microdissection of foregut endoderm from (anterior) thyroid region, (mid) lung region, and (posterior) liver/pancreas region from embryos containing 21–25 somites. (Before) picture of a transverse tissue section before laser capture, (after) tissue remaining on the slide after dissection, (cap) tissue collected on the cap membrane. Nt, notochord; Fg, foregut; Th, thyroid bud; Li, Liver bud; H, heart. (b) Real-time RT-PCR of three selected transcription factors that show distinctive patterns of expression along anterior (A), mid (M), and posterior (P) foregut endoderm from 21 to 25 somite embryos. (c) Real-time RT-PCR of three selected transcription genes that show distinctive patterns of expression along anterior (A), mid (M) and posterior (P) foregut endoderm from 26 to 30 somite embryos.

the posterior region, although it is expressed in other regions of the foregut.

1.8. Patterns of expression of genes identified in the microarray analysis

To further validate the microarray data we analyzed by whole mount in situ hybridization the pattern of expression of a number of genes involved in regulation of transcription. The transcription factor Isl1 is significantly up-regulated in the mid-foregut at the time of lung bud formation by microarray and QRT-PCR analyses. Whole mount in situ hybridization performed in 26–30 somite embryos (E9.5) (Fig. 6A and B) showed the presence of Isl1 mRNA in primary lung-bud mesenchyme. Although at this stage Isl1 is no longer expressed in cardiac cells, it can be detected in the sinus venosus (Fig. 6A). Expression is also high in the stomach region (Fig. 6B). Isl1 is essential for motor neuron differentiation and normal development of the heart, pancreas, and splanchnic mesenchyme, but

its importance in lung development is not known due to the early lethal phenotype of the Isl1 null mutant mice (Ahlgren et al., 1997; Cai et al., 2003; Pfaff et al., 1996; Thaler et al., 2004). Assessment of Isl1 expression by QRT-PCR in total lung at different developmental time points shows that Isl1 expression is transient, since the mRNA level peaks on embryonic day E9.5 and decreases at E11.5 to that of E8.5 (Fig. 6C). This is followed by a gradual decline during later

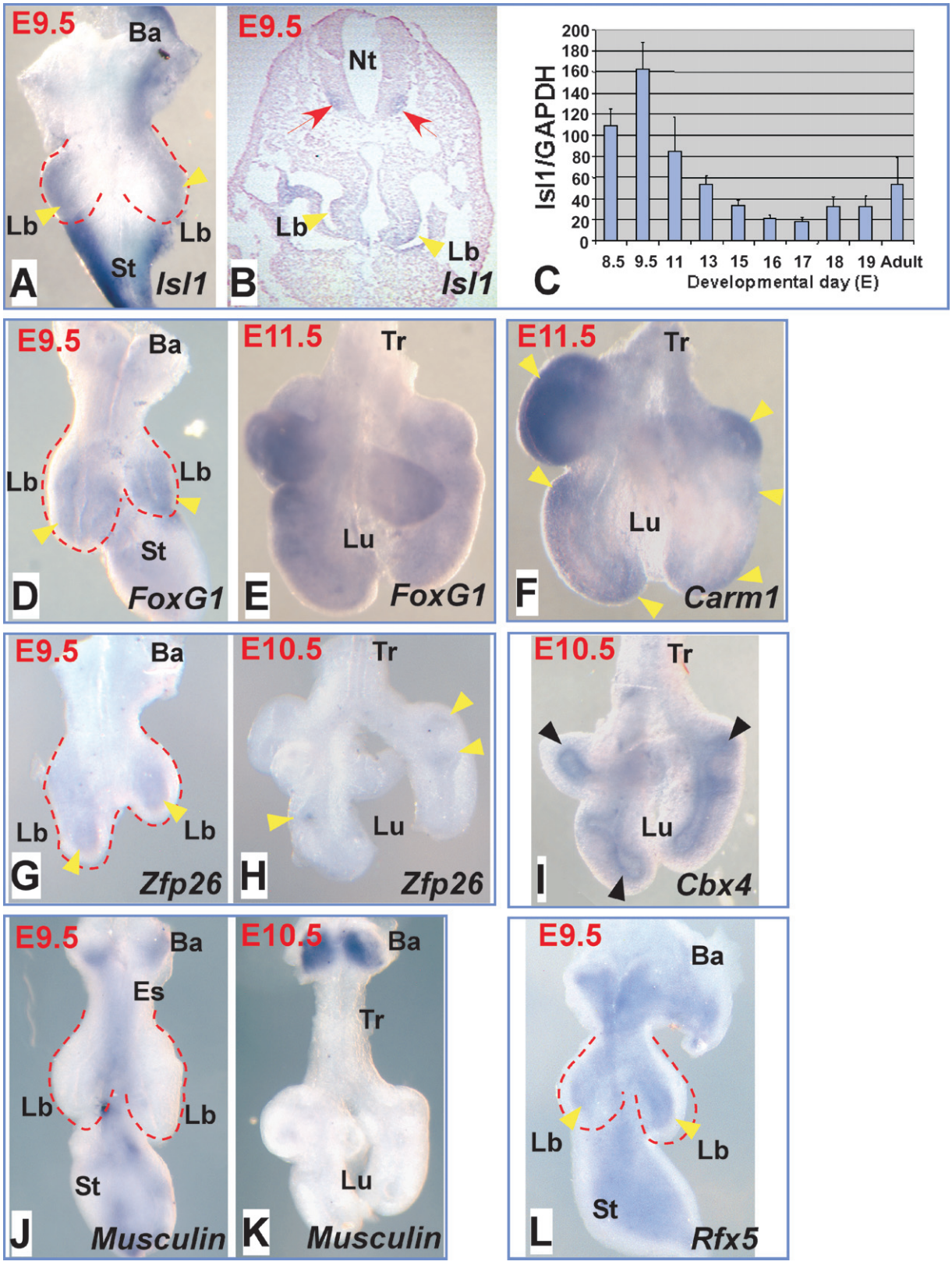

development to levels that are about 10–15% of the peak value. Isl1 continue to be detected in adult lung although the levels are lower than the ones observed during lung budding.

Expression of FoxG1 was localized in the mesenchyma of the primary lung buds at E9.5 and in the lung mesenchyme at E11.5 (Fig. 6D and E). FoxG1 is a forkhead transcription factor involved in morphogenesis of the telencephalon by controlling proliferation and differentiation of precursor cells (Martynoga et al., 2005). It participates in different signaling pathways. FoxG1 interferes with TGFβ pathway by association with Smad-interacting proteins (Seoane et al., 2004); it also interacts with the delta/notch/hes pathway by combining with Hes homodimers to repress transcription (Yao et al., 2001).

Two genes involved in chromatin modification Carm1 and Cbx4, identified in the microarray analysis, were barely detected by whole mount in situ hybridization in the primary buds at E9.5 (data not shown). Their expression, though, is highly increased by E11.5. Carm 1 is concentrated in mesenchymal cells at the tips of the lung branches (Fig. 6F), while Cbx4 is in the epithelium (Fig. 6I). Carm1 (coactivator associated arginine methyltransferase) is a transcriptional activator that interacts with the p160 family of nuclear receptor-associated factors and methylates histone 3 at arginine 17. Methylation of arginines by Carm1 occurs along with acetylation of histones to remodel chromatin and recruit RNA polymerase II (Teyssier et al., 2002). Cbx4 (Chromobox homolog 4) is one of the five mouse Polycomb homologs that act as transcriptional repressors. Cbx4 binds to chromatin preferentially to histone 3 trimethylated in lysine 9 (H3K9me3) (Bernstein et al., 2006) and promotes SUMOylation of transcriptional repressors such as the DNA methyltransferase Dnmt3a (Li et al., 2007). Three other transctiption factors Zfp26 (Chowdhury et al., 1988), musculin (Lu et al., 1999), and Rfx5 (Xu et al., 2007) that are up-regulated in the mid-foregut during lung budding (Table 1) can also be detected by whole mount in situ hybridization at E9.5 in a very distinctive pattern. Zfp26, a zinc-finger transcription factor is detected in the sub-epithelial mesenchyme of the primary buds (Fig. 6G). At E10.5 it is barely detected with some expression remaining at the tips of the forming branches (Fig. 6H). Musculin, or MyoR, a repressor of muscle differentiation that competes with the myogenic factor MyoD, is expressed in the mid-region of the foregut, in particular in the esophagus, but it is not expressed in the primary lung buds (Fig. 6J). Expression can be detected also in the branchial arches and the stomach. The branchial arches continue to be positive at E10.5 and the lung is negative (Fig. 6K). In contrast Rfx5 is expressed in mesenchymal cells of the branchial arches, primary lung buds and stomach in the sub-epithelial layer (Fig. 6L). Expression of Zbtb1, Ing3, Rbbp4, and Smarce 1 was detected in the mid-region of the foregut and/or whole embryos at E9.5 by whole mount in situ hybridization but they are ubiquitously expressed (data not shown).

1.9. Concluding remarks

In this study we have characterized the transcriptome of the mid-region of the mouse foregut during the period between lung specification of foregut cells and appearance of the initial lung buds. We have identified a substantial number of genes present in the prospective lung region, and genes that change their level of expression as the lung bud forms. We selected, for further studies, those involved in regulation of transcription since they were overrepresented among the genes that change as the lung forms, and because these factors likely activate the developmental program that sustains lung formation. The information generated, therefore, expands the list of genes to study new and known pathways driving lung progenitor cell differentiation and lung morphogenesis.

2. Experimental procedures

2.1. Isolation of mid-foregut tissue

We selected based on morphological features, three developmental stages to study gene expression profiles of mid-foregut tissue, containing endoderm and mesoderm cells. The stages are: 16–20 somite embryos, 21–25 somite embryos and 25–30 somite embryos. The earliest samples (16–20 somites) show evidence of primitive thyroid and liver/pancreas budding which provide morphologic limits at the extremes of the mid-foregut field from which the lung is derived. All embryos with greater than 25 somites have initiated formation of bilateral lung buds. Although some variability is expected in the relationship between somite number and mor-

Fig. 6. Pattern of expression of selected genes in the primary lung buds and developing lung determined by whole mount in situ hybridization. (A) Isl1 is mainly expressed in the mesenchyme of the primary lung buds (yellow arrowheads) and the stomach of embryonic foreguts at E9.5. (B) Transverse section of paraffin embedded whole embryos after WMISH, counter stained with Fast Red, shows expression of Isl1 in the neural tube (red arrows), the tips of the forming lung buds and the sinus venosus at E9.5 (yellow arrowheads). (C) Expression of Isl1 mRNA was also determined by real-time RT-PCR at different stages of lung development and in adult lung. Isl1 expression level is normalized to GAPDH. $n = 3$. Error bars represent standard error of the mean. (D) FoxG1 is expressed in the mesenchyme of the primary lung buds (yellow arrowheads) and stomach at E9.5. (E) FoxG1 is diffusely detected in the lung mesenchyme at E11.5. (F) Carm1 is concentrated in the mesenchyme at the tips of the lung branches at E11.5 (yellow arrowheads). (G) Zfp26 is expressed in the mesenchyme close to the epithelium in the forming primary buds at E9.5 (yellow arrowheads). (H) Zfp26 is faintly detected at the tips of the branches at E10.5 (yellow arrowheads). (I) Cbx4 is expressed in the epithelium of the lung branches at E10.5 (black arrowheads). (J) Musculin is absent in the primary lung buds at E9.5 but is expressed in the mid foregut along the esophagus. It is also expressed in the branchial arches and stomach, likely in muscle progenitor cells. (K) Musculin is not detected in the lung at E10.5 but expression continues in the branchial arches. (L) Rfx5 is expressed in the subepithelial mesenchyme alongside the foregut, including the primary lung buds at E9.5 (yellow arrowheads). Fg, foregut; Nt, neural tube; H, heart, Sv, sinus venosus; Ba, branchial arches; Lb, primary lung bud; Lu, lung; Tr, trachea.

phology, there is a high degree of uniformity within the range of number of somites used to group the earliest and latest samples for molecular analysis.

Pregnant CD-1 mice were purchased from Charles River with pregnancy timed by the presence of a vaginal plug at day E0.5 of gestation. Dams were sacrificed at 6–12 h intervals between gestational days E8.5 and E10 to obtain embryos containing between 16 and 30 somites. After hysterotomy, embryos were placed in PBS at 4 °C prior to dissection. Each embryo was examined by dissecting microscopy to determine its somite number. Embryos were divided into three groups according to somite number: 16–20, 21–25, and 26–30 somites. This grouping correlates well with morphological features described above: 16–20 somite embryos have thyroid and liver buds but lack lung buds; all 26–30 somite embryos have lung, thyroid, and liver buds. The 20–25 somite group includes a small number of embryos in which lung buds have just commenced to emerge but are difficult to visualize. To obtain mid-foregut tissue, the neural tube and heart were dissected away for the embryo to expose the foregut. The foregut tissue posterior to the pharyngeal arches and anterior to the liver was excised using tungsten needles. Collected tissues were placed immediately in RNeasy™ buffer (Qiagen). Five to 10 mid-foreguts were pooled for each of the three somite groups for RNA analysis.

For histological analysis embryos or isolated mid-foreguts were fixed in 4% freshly prepared paraformaldehyde in PBS, stored in fixative overnight at 4 °C, and embedded in paraffin following standard processing with ethanol dehydration. For laser capture microdissection embryos were fixed in 70% alcohol overnight at 4 °C, dehydrated and embedded in paraffin in RNAse-free conditions (Goldsworthy et al., 1999). Paraffin blocks were examined in a dissecting microscope with fiberoptic lighting to determine the orientation of the embryo. Excess paraffin was trimmed away, and the embryo was then reembedded oriented in a supine position (ventral side up). Six micron transverse sections were prepared for further study.

2.2. RNA purification and amplification and microarray quality controls

Total RNA was isolated from dissected tissues using RNeasy™ micropurification kit (Qiagen) according to the manufacturer's directions, followed by treatment on column with DNA-*free*™ DNase (Ambion). RNA concentrations were measured in 1 μl (1/10 of the sample) in a NanoDrop ND-1000 spectrophotometer (NanoDrop Technologies). RNA (100 ng) was amplified using the RiboAmp HS kit (Arcturus Engineering, Inc.) as described by the manufacturer. RNA was labelled using biotinylated ribonucleotides during the second *in vitro* transcription step using ENZO kit (Affymetrix). After two rounds of amplification, 10–15 μg of amplified RNA (aRNA) were obtained. The quality of amplified RNA obtained from microdissected foreguts was evaluated by examining the size distribution of the aRNA and aRNA from E18.5 fetal lung, used as control, in an agarose gel stained with Sybr Gold (Molecular Probes). A similar size distribution of aRNA in the three samples, ranging from ~200 bp to >2 kb is shown in (Fig. S2A, supplementary material). Thus the handling and time required for isolation of the samples has not resulted in degraded RNA unsuitable for microarray hybridization. Acceptable correlation values (R^2) values indicating reproducibility of microarrays are shown in Fig. S2B (technical replicates $R^2 = 0.973$) and Fig. S2C (biological replicates $R^2 = 0.969$) in Supplementary material.

2.3. Microarray experiments

Gene expression profiles of three independent mRNA samples for each of the three somite number groups were determined using MOE430 A2.0 microarrays (Affymetrix), containing 22,690 probe sets. Genes represented on this array are available at http://www.affymetrix.com/products/arrays/specific/mouse430_2.affx. Each scanned image was evaluated for significant artifacts. Bacterial genes spiked into the hybridization mixture (bioB and bioC) were used as positive quality controls for hybridization procedures. Arrays showing similar quality control parameters (Table S1, supplementary material) were used for data analysis. Background and noise measurements were below 100 in all arrays. The average ratio of signals from mid-sequence and 3′ probe sets for GAPDH and actin was consistent within all arrays, indicating similar efficiency of the amplification step. This allows comparison of amplified genes between independent arrays. As expected these ratios were higher than in non-amplified samples due to the preferential amplification of the 3′ end of the mRNA using polydT. Minimal degradation of the isolated mRNA could have occurred, even though strict RNAse-free conditions were used in every step of the experiments to avoid this problem. Data from each array was scaled (target intensity of 100) to normalize the results for inter-array comparisons. Reproducibility of the amplification and hybridization experiments was determined by correlation analysis of the microarray data obtained in replicates of 26–30 somite foregut RNA, starting from the same RNA (technical replicates) or from RNA from different embryos (biological replicates).

2.4. Microarray data analyses

A single weighted mean expression level for each gene was derived using Microarray Suite (MAS) 5.0 software (Affymetrix). Using a one-sided Wilcoxon signed-rank test, the MAS 5.0 software generated a detection *p*-value for each gene indicating whether or not the transcript was reliably detected. An initial mild filter was applied to select genes with detection *p*-value less than 0.05 in at least one of the nine arrays. A total of 13,371 probe sets passed the filter and were used in further statistical analyses. A parametric ANOVA was performed to find genes differentially expressed between two or more of the groups. One-thousand seventy-six genes passed the ANOVA test at $p < 0.05$, a significantly larger number than expected by chance (650 genes would be expected by chance). 80% of the 1076 genes were indeed detected in more than seven arrays of the nine arrays analyzed. While a significant proportion of genes identified on statistical analysis may represent false positives, we limited our biological analysis to those whose fold changes were greater than 1.8-fold. In addition, a large number of biologically relevant genes were validated by other methods. We performed a K-means clustering analysis with the 1076 genes that passed the ANOVA test ($p \leqslant 0.05$), to determine groups of genes that have similar time course profiles of expression levels over the three time points studied. To make the different genes comparable to each other in the cluster groups, the average of each sample group was calculated and *z*-score-normalized so the mean of the averages is zero and the standard deviation is one. K-means clustering was performed in Spotfire DecisionSite arbitrarily setting the number of clusters (k) equal to five. This method allows the identification of genes enriched in each of the somite groups. A Student's *t* tests was also performed ($p \leqslant 0.05$) to compare the earliest vs. the latest time point (16–20 somites to 26–30 somites). We used EASE (Expression Analysis Systematic Explorer), http://david.abcc.ncifcrf.gov/ease/ease.jsp, and the GO functional classification database to discover enriched biological themes within the lists of genes which are increased or decreased (>1.8-fold) as the lung bud forms (16–20 somite samples vs. 26–30 somite samples). We have opted to use 1.8-fold as cut-off level due to the high number of genes showing a statistically significant change between 1.8- and 2-fold. The genes used in the EASE analysis pass ANOVA ($p \leqslant 0.05$) and Student's *t* tests ($p \leqslant 0.05$). EASE analyzes a list of Affymetrix ID numbers of the genes under study (input list) and finds over-represented biological "themes" in the list of genes, compared to the total number of genes for each biological theme in the array. The significance of each category is determined by two statistical values that are used to sort the categories i.e. the standard Fisher exact probability, and a conservative EASE score that identifies robust categories. We considered categories with an EASE score $\leqslant 0.05$ as over-represented.

2.5. Real-time RT-PCR

Selected genes identified as differentially expressed in the mid-foregut by microarray analysis were validated by real-time RT-PCR (QRT-PCR) in non-amplified mid-foregut RNA samples. Total non-amplified

RNA from embryonic mid-foreguts grouped as before was treated with DNA-*free*™ DNase (Ambion) and reversed transcribed (RT) (1 μg of RNA in 25 μl reaction volume) using AMV reverse transcriptase (Promega). RT reactions, diluted appropriately to obtain a signal in fewer than 34 cycles, were analyzed by QRT-PCR in an ABI 7000 Sequence Detection System (Applied Biosystems). PrimerExpress software version 2.0 (Applied Biosystems) was used to design primers for SybrGreen reactions, while TaqMan primers and probes used were Assays-on-Demand (Applied Biosystems) (Table S2, supplementary material). Reactions were performed in 50 μl using SybrGreen PCR master mix or TaqMan PCR universal master mix (Applied Biosystems). Optimal reaction conditions were determined for all primers and probes and dissociation curves were generated for primers used in SybrGreen reactions to confirm a single PCR amplification product. A calibration curve, generated with serial dilutions of reverse transcribed E18.5 total lung or E8.5 total embryo RNA ($n = 3$), was used to determine the relative message concentration for each gene tested. Data were normalized to relative concentration of GAPDH mRNA amplified from the same RT reaction. Using equal amounts of total RNA from 16 to 20, 21 to 25, and 26 to 30 somite groups we established that the relative expression level of GAPDH is similar at all three time points (data not shown). GAPDH was therefore used to normalize gene expression in QRT-PCR experiments.

2.6. Whole mount in situ hybridization

Whole mount in situ hybridization was performed as described by Wilkinson (Xu and Wilkinson, 1998) and modified by Desai et al. (2004). Anti-sense and sense probes were generated by RT-PCR using oligonucleotides containing adaptors for T3 or T7 promoters (see oligonucleotide sequences in Table S8, supplementary material). Purified PCR fragments were used as templates in the *in vitro* transcription reaction (Maxiscript kit, Ambion) to synthetize sense and antisense riboprobes labeled with digoxigenin (DIG). After hybridization and staining of the embryos with BMpurple (Boehringer Mannheim), some were dehydrated and embedded in paraffin. Transverse sections (10 μm) were obtained as described above, and counterstained with Fast Red using standard methods.

2.7. Laser capture microdissection (LCM) of foregut endoderm

We isolated endoderm cells from the anterior (thyroid region), mid (lung region) and posterior (liver/pancreas region) foregut of 21–25 and 26–30 somite embryos by laser capture microdissection. Embryos were fixed, embedded, and oriented in a supine position as described above. Six micron transverse sections were placed on plain glass slides, dried for 30 min at 37 °C and immediately deparaffinized and dehydrated in xylenes (2×5 min), absolute ethanol (30s) and xylenes (2×5 min). Slides were dried at room temperature for 10 min and placed in slide boxes containing Drierite to keep them dry while dissecting. Foregut endoderm was microdissected using a PixCell I laser capture microdisection system (Arcturus) with a laser spot size of 30 μ, pulse power 15 mW, pulse width 15.2 ms. Sections from two embryos were collected per CapSure LCM cap (Arcturus) and total RNA was purified as described above. RNA purified from 6 to 10 embryos was pooled for QRT-PCR and [^{32}P]RT-PCR analyses.

Acknowledgements

We thank Drs. Mary C. Williams, Jerome S. Brody, Wellington V. Cardoso, and YuXia Cao for thoughtful comments about the manuscript. Dr. Norman Gerry for his technical support in the microarray data analysis. This work was supported by NHLBI Program Project Grant HL47049, and Doris Duke Charitable Foundation Clinical Scientist Development Award (A.S.).

Appendix A. Supplementary data

Supplementary data associated with this article can be found, in the online version, at doi:10.1016/j.modgep.2007.09.003.

References

Ahlgren, U., Pfaff, S.L., Jessell, T.M., Edlund, T., Edlund, H., 1997. Independent requirement for ISL1 in formation of pancreatic mesenchyme and islet cells. Nature 385, 257–260.

Aitola, M., Carlsson, P., Mahlapuu, M., Enerback, S., Pelto-Huikko, M., 2000. Forkhead transcription factor FoxF2 is expressed in mesodermal tissues involved in epithelio-mesenchymal interactions. Dev. Dyn. 218, 136–149.

Ang, S.L., Rossant, J., 1994. HNF-3 beta is essential for node and notochord formation in mouse development. Cell 78, 561–574.

Banerjee, S.K., Young, H.W., Barczak, A., Erle, D.J., Blackburn, M.R., 2004. Abnormal alveolar development associated with elevated adenine nucleosides. Am. J. Respir. Cell Mol. Biol. 30, 38–50.

Bellusci, S., Furuta, Y., Rush, M.G., Henderson, R., Winnier, G., Hogan, B.L., 1997. Involvement of Sonic hedgehog (Shh) in mouse embryonic lung growth and morphogenesis. Development 124, 53–63.

Bernstein, E., Duncan, E.M., Masui, O., Gil, J., Heard, E., Allis, C.D., 2006. Mouse polycomb proteins bind differentially to methylated histone H3 and RNA and are enriched in facultative heterochromatin. Mol. Cell. Biol. 26, 2560–2569.

Bonner, A.E., Lemon, W.J., You, M., 2003. Gene expression signatures identify novel regulatory pathways during murine lung development: implications for lung tumorigenesis. J. Med. Genet. 40, 408–417.

Bort, R., Signore, M., Tremblay, K., Martinez Barbera, J.P., Zaret, K.S., 2006. Hex homeobox gene controls the transition of the endoderm to a pseudostratified, cell emergent epithelium for liver bud development. Dev. Biol. 290, 44–56.

Cai, C.L., Liang, X., Shi, Y., Chu, P.H., Pfaff, S.L., Chen, J., Evans, S., 2003. Isl1 identifies a cardiac progenitor population that proliferates prior to differentiation and contributes a majority of cells to the heart. Dev. Cell 5, 877–889.

Cardoso, W.V., 1995. Transcription factors and pattern formation in the developing lung. Am. J. Physiol. 269, L429–L442.

Cardoso, W.V., Lu, J., 2006. Regulation of early lung morphogenesis: questions, facts and controversies. Development 133, 1611–1624.

Carlsson, P., Mahlapuu, M., 2002. Forkhead transcription factors: key players in development and metabolism. Dev. Biol. 250, 1–23.

Chaudhry, A.Z., Lyons, G.E., Gronostajski, R.M., 1997. Expression patterns of the four nuclear factor I genes during mouse embryogenesis indicate a potential role in development. Dev. Dyn. 208, 313–325.

Chen, J., Archer, T.K., 2005. Regulating SWI/SNF subunit levels via protein–protein interactions and proteasomal degradation: BAF155 and BAF170 limit expression of BAF57. Mol. Cell. Biol. 25, 9016–9027.

Chowdhury, K., Rohdewohld, H., Gruss, P., 1988. Specific and ubiquitous expression of different Zn finger protein genes in the mouse. Nucleic Acids Res. 16, 9995–10011.

Cleaver, O., Krieg, P.A., 2001. Notochord patterning of the endoderm. Dev. Biol. 234, 1–12.

Cohen, D.R., Cheng, C.W., Cheng, S.H., Hui, C.C., 2000. Expression of two novel mouse Iroquois homeobox genes during neurogenesis. Mech. Dev. 91, 317–321.

Costa, R.H., Kalinichenko, V.V., Lim, L., 2001. Transcription factors in mouse lung development and function. Am. J. Physiol. Lung. Cell Mol. Physiol. 280, L823–L838.

David, G., Bai, X.M., Van der Schueren, B., Marynen, P., Cassiman, J.J., Van den Berghe, H., 1993. Spatial and temporal changes in the expression of fibroglycan (syndecan-2) during mouse embryonic development. Development 119, 841–854.

Davis, R.J., Shen, W., Sandler, Y.I., Heanue, T.A., Mardon, G., 2001. Characterization of mouse Dach2, a homologue of *Drosophila dachshund*. Mech. Dev. 102, 169–179.

DeFelice, M., Silberschmidt, D., DiLauro, R., Xu, Y., Wert, S.E., Weaver, T.E., Bachurski, C.J., Clark, J.C., Whitsett, J.A., 2003. TTF-1 phosphorylation is required for peripheral lung morphogenesis, perinatal survival, and tissue-specific gene expression. J. Biol. Chem. 278, 35574–35583.

Desai, T.J., Malpel, S., Flentke, G.R., Smith, S.M., Cardoso, W.V., 2004. Retinoic acid selectively regulates Fgf10 expression and maintains cell identity in the prospective lung field of the developing foregut. Dev. Biol. 273, 402–415.

Domingos, P.M., Obukhanych, T.V., Altmann, C.R., Hemmati-Brivanlou, A., 2002. Cloning and developmental expression of Baf57 in *Xenopus laevis*. Mech. Dev. 116, 177–181.

Doyon, Y., Selleck, W., Lane, W.S., Tan, S., Cote, J., 2004. Structural and functional conservation of the NuA4 histone acetyltransferase complex from yeast to humans. Mol. Cell. Biol. 24, 1884–1896.

Francis, R., McGrath, G., Zhang, J., Ruddy, D.A., Sym, M., Apfeld, J., Nicoll, M., Maxwell, M., Hai, B., Ellis, M.C., Parks, A.L., Xu, W., Li, J., Gurney, M., Myers, R.L., Himes, C.S., Hiebsch, R., Ruble, C., Nye, J.S., Curtis, D., 2002. aph-1 and pen-2 are required for Notch pathway signaling, gamma-secretase cleavage of betaAPP, and presenilin protein accumulation. Dev. Cell 3, 85–97.

Ganapathi, M.K., Kwon, M., Haney, P.M., McTiernan, C., Javed, A.A., Pepin, R.A., Samols, D., Patel, M.S., 1987. Cloning of rat brain succinyl-CoA:3-oxoacid CoA-transferase cDNA. Regulation of the mRNA in different rat tissues and during brain development. Biochem. J. 248, 853–857.

Goldsworthy, S.M., Stockton, P.S., Trempus, C.S., Foley, J.F., Maronpot, R.R., 1999. Effects of fixation on RNA extraction and amplification from laser capture microdissected tissue. Mol. Carcinog. 25, 86–91.

Grapin-Botton, A., Melton, D.A., 2000. Endoderm development: from patterning to organogenesis. Trends Genet. 16, 124–130.

Gu, G., Wells, J.M., Dombkowski, D., Preffer, F., Aronow, B., Melton, D.A., 2004. Global expression analysis of gene regulatory pathways during endocrine pancreatic development. Development 131, 165–179.

Horb, M.E., 2000. Patterning the endoderm: the importance of neighbours. Bioessays 22, 599–602.

Jeong, J.W., Lee, K.Y., Kwak, I., White, L.D., Hilsenbeck, S.G., Lydon, J.P., DeMayo, F.J., 2005. Identification of murine uterine genes regulated in a ligand-dependent manner by the progesterone receptor. Endocrinology 146, 3490–3505.

Jung, J., Zheng, M., Goldfarb, M., Zaret, K.S., 1999. Initiation of mammalian liver development from endoderm by fibroblast growth factors. Science 284, 1998–2003.

Khoor, A., Stahlman, M.T., Gray, M.E., Whitsett, J.A., 1994. Temporal-spatial distribution of SP-B and SP-C proteins and mRNAs in developing respiratory epithelium of human lung. J. Histochem. Cytochem. 42, 1187–1199.

Kim, I.M., Ramakrishna, S., Gusarova, G.A., Yoder, H.M., Costa, R.H., Kalinichenko, V.V., 2005. The forkhead box m1 transcription factor is essential for embryonic development of pulmonary vasculature. J. Biol. Chem. 280, 22278–22286.

Kimura, S., Ward, J.M., Minoo, P., 1999. Thyroid-specific enhancer-binding protein/thyroid transcription factor 1 is not required for the initial specification of the thyroid and lung primordia. Biochimie 81, 321–327.

Kitamura, T., Nakae, J., Kitamura, Y., Kido, Y., Biggs 3rd, W.H., Wright, C.V., White, M.F., Arden, K.C., Accili, D., 2002. The forkhead transcription factor Foxo1 links insulin signaling to Pdx1 regulation of pancreatic beta cell growth. J. Clin. Invest. 110, 1839–1847.

Kumar, M., Jordan, N., Melton, D., Grapin-Botton, A., 2003. Signals from lateral plate mesoderm instruct endoderm toward a pancreatic fate. Dev. Biol. 259, 109–122.

Ladi, E., Nichols, J.T., Ge, W., Miyamoto, A., Yao, C., Yang, L.T., Boulter, J., Sun, Y.E., Kintner, C., Weinmaster, G., 2005. The divergent DSL ligand Dll3 does not activate Notch signaling but cell autonomously attenuates signaling induced by other DSL ligands. J. Cell Biol. 170, 983–992.

Lakhani, S.A., Masud, A., Kuida, K., Porter Jr., G.A., Booth, C.J., Mehal, W.Z., Inayat, I., Flavell, R.A., 2006. Caspases 3 and 7: key mediators of mitochondrial events of apoptosis. Science 311, 847–851.

Lee, C.S., Friedman, J.R., Fulmer, J.T., Kaestner, K.H., 2005. The initiation of liver development is dependent on Foxa transcription factors. Nature 435, 944–947.

Lee, T.I., Jenner, R.G., Boyer, L.A., Guenther, M.G., Levine, S.S., Kumar, R.M., Chevalier, B., Johnstone, S.E., Cole, M.F., Isono, K., Koseki, H., Fuchikami, T., Abe, K., Murray, H.L., Zucker, J.P., Yuan, B., Bell, G.W., Herbolsheimer, E., Hannett, N.M., Sun, K., Odom, D.T., Otte, A.P., Volkert, T.L., Bartel, D.P., Melton, D.A., Gifford, D.K., Jaenisch, R., Young, R.A., 2006. Control of developmental regulators by Polycomb in human embryonic stem cells. Cell 125, 301–313.

Lemaigre, F., Zaret, K.S., 2004. Liver development update: new embryo models, cell lineage control, and morphogenesis. Curr. Opin. Genet. Dev. 14, 582–590.

Li, B., Zhou, J., Liu, P., Hu, J., Jin, H., Shimono, Y., Takahashi, M., Xu, G., 2007. Polycomb protein Cbx4 promotes SUMO modification of de novo DNA methyltransferase Dnmt3a. Biochem. J. 405, 369–378.

Li, E., 2002. Chromatin modification and epigenetic reprogramming in mammalian development. Nat. Rev. Genet. 3, 662–673.

Li, H., Arber, S., Jessell, T.M., Edlund, H., 1999. Selective agenesis of the dorsal pancreas in mice lacking homeobox gene Hlxb9. Nat. Genet. 23, 67–70.

Litingtung, Y., Lei, L., Westphal, H., Chiang, C., 1998. Sonic hedgehog is essential to foregut development. Nat. Genet. 20, 58–61.

Louvi, A., Artavanis-Tsakonas, S., 2006. Notch signalling in vertebrate neural development. Nat. Rev. Neurosci. 7, 93–102.

Lu, J., Izvolsky, K.I., Qian, J., Cardoso, W.V., 2005. Identification of FGF10 targets in the embryonic lung epithelium during bud morphogenesis. J. Biol. Chem. 280, 4834–4841.

Lu, J., Qian, J., Izvolsky, K.I., Cardoso, W.V., 2004a. Global analysis of genes differentially expressed in branching and non-branching regions of the mouse embryonic lung. Dev. Biol. 273, 418–435.

Lu, J., Webb, R., Richardson, J.A., Olson, E.N., 1999. MyoR: a muscle-restricted basic helix-loop-helix transcription factor that antagonizes the actions of MyoD. Proc. Natl. Acad. Sci. USA 96, 552–557.

Lu, T., Pan, Y., Kao, S.Y., Li, C., Kohane, I., Chan, J., Yankner, B.A., 2004b. Gene regulation and DNA damage in the ageing human brain. Nature 429, 883–891.

Martynoga, B., Morrison, H., Price, D.J., Mason, J.O., 2005. Foxg1 is required for specification of ventral telencephalon and region-specific regulation of dorsal telencephalic precursor proliferation and apoptosis. Dev. Biol. 283, 113–127.

Matsumoto, K., Yoshitomi, H., Rossant, J., Zaret, K.S., 2001. Liver organogenesis promoted by endothelial cells prior to vascular function. Science 294, 559–563.

McReynolds, M.R., Taylor-Garcia, K.M., Greer, K.A., Hoying, J.B., Brooks, H.L., 2005. Renal medullary gene expression in aquaporin-1 null mice. Am. J. Physiol. Ren. Physiol. 288, F315–F321.

Murtaugh, L.C., Melton, D.A., 2003. Genes, signals, and lineages in pancreas development. Annu. Rev. Cell Dev. Biol. 19, 71–89.

Ohuchi, H., Yasue, A., Ono, K., Sasaoka, S., Tomonari, S., Takagi, A., Itakura, M., Moriyama, K., Noji, S., Nohno, T., 2005. Identification of cis-element regulating expression of the mouse Fgf10 gene during inner ear development. Dev. Dyn. 233, 177–187.

Packer, A.I., Mailutha, K.G., Ambrozewicz, L.A., Wolgemuth, D.J., 2000. Regulation of the Hoxa4 and Hoxa5 genes in the embryonic mouse lung by retinoic acid and TGFbeta1: implications for lung development and patterning. Dev. Dyn. 217, 62–74.

Parlato, R., Rosica, A., Rodriguez-Mallon, A., Affuso, A., Postiglione, M.P., Arra, C., Mansouri, A., Kimura, S., Di Lauro, R., De Felice, M., 2004. An integrated regulatory network controlling survival and migration in thyroid organogenesis. Dev. Biol. 276, 464–475.

Pfaff, S.L., Mendelsohn, M., Stewart, C.L., Edlund, T., Jessell, T.M., 1996. Requirement for LIM homeobox gene Isl1 in motor neuron generation reveals a motor neuron-dependent step in interneuron differentiation. Cell 84, 309–320.

Ramirez, M.I., Pollack, L., Millien, G., Cao, Y.X., Hinds, A., Williams, M.C., 2002. The alpha-isoform of caveolin-1 is a marker of vasculogenesis in early lung development. J. Histochem. Cytochem. 50, 33–42.

Ringrose, L., Paro, R., 2004. Epigenetic regulation of cellular memory by the Polycomb and Trithorax group proteins. Annu. Rev. Genet. 38, 413–443.

Rossi, J.M., Dunn, N.R., Hogan, B.L., Zaret, K.S., 2001. Distinct mesodermal signals, including BMPs from the septum transversum mesenchyme, are required in combination for hepatogenesis from the endoderm. Genes Dev. 15, 1998–2009.

Sakiyama, J., Yamagishi, A., Kuroiwa, A., 2003. Tbx4-Fgf10 system controls lung bud formation during chicken embryonic development. Development 130, 1225–1234.

Sekine, K., Ohuchi, H., Fujiwara, M., Yamasaki, M., Yoshizawa, T., Sato, T., Yagishita, N., Matsui, D., Koga, Y., Itoh, N., Kato, S., 1999. Fgf10 is essential for limb and lung formation. Nat. Genet. 21, 138–141.

Seoane, J., Le, H.V., Shen, L., Anderson, S.A., Massague, J., 2004. Integration of Smad and forkhead pathways in the control of neuroepithelial and glioblastoma cell proliferation. Cell 117, 211–223.

Serls, A.E., Doherty, S., Parvatiyar, P., Wells, J.M., Deutsch, G.H., 2005. Different thresholds of fibroblast growth factors pattern the ventral foregut into liver and lung. Development 132, 35–47.

Sherwood, R.I., Jitianu, C., Cleaver, O., Shaywitz, D.A., Lamenzo, J.O., Chen, A.E., Golub, T.R., Melton, D.A., 2007. Prospective isolation and global gene expression analysis of definitive and visceral endoderm. Dev. Biol. 304, 541–555.

Shu, W., Yang, H., Zhang, L., Lu, M.M., Morrisey, E.E., 2001. Characterization of a new subfamily of winged-helix/forkhead (Fox) genes that are expressed in the lung and act as transcriptional repressors. J. Biol. Chem. 276, 27488–27497.

Sudarsanam, P., Winston, F., 2000. The Swi/Snf family nucleosome-remodeling complexes and transcriptional control. Trends Genet. 16, 345–351.

Taichman, D.B., Loomes, K.M., Schachtner, S.K., Guttentag, S., Vu, C., Williams, P., Oakey, R.J., Baldwin, H.S., 2002. Notch1 and Jagged1 expression by the developing pulmonary vasculature. Dev. Dyn. 225, 166–175.

Teyssier, C., Chen, D., Stallcup, M.R., 2002. Requirement for multiple domains of the protein arginine methyltransferase CARM1 in its transcriptional coactivator function. J. Biol. Chem. 277, 46066–46072.

Thaler, J.P., Koo, S.J., Kania, A., Lettieri, K., Andrews, S., Cox, C., Jessell, T.M., Pfaff, S.L., 2004. A postmitotic role for Isl-class LIM homeodomain proteins in the assignment of visceral spinal motor neuron identity. Neuron 41, 337–350.

Thor, S., Ericson, J., Brannstrom, T., Edlund, T., 1991. The homeodomain LIM protein Isl-1 is expressed in subsets of neurons and endocrine cells in the adult rat. Neuron 7, 881–889.

Tremblay, K.D., Zaret, K.S., 2005. Distinct populations of endoderm cells converge to generate the embryonic liver bud and ventral foregut tissues. Dev. Biol. 280, 87–99.

Trueba, S.S., Auge, J., Mattei, G., Etchevers, H., Martinovic, J., Czernichow, P., Vekemans, M., Polak, M., Attie-Bitach, T., 2005. PAX8, TITF1, and FOXE1 gene expression patterns during human development: new insights into human thyroid development and thyroid dysgenesis-associated malformations. J. Clin. Endocrinol. Metab. 90, 455–462.

Wang, J., Souza, P., Kuliszewski, M., Tanswell, A.K., Post, M., 1994. Expression of surfactant proteins in embryonic rat lung. Am. J. Respir. Cell Mol. Biol. 10, 222–229.

Wang, T., Tamakoshi, T., Uezato, T., Shu, F., Kanzaki-Kato, N., Fu, Y., Koseki, H., Yoshida, N., Sugiyama, T., Miura, N., 2003. Forkhead transcription factor Foxf2 (LUN)-deficient mice exhibit abnormal development of secondary palate. Dev. Biol. 259, 83–94.

Warburton, D., Bellusci, S., De Langhe, S., Del Moral, P.M., Fleury, V., Mailleux, A., Tefft, D., Unbekandt, M., Wang, K., Shi, W., 2005. Molecular mechanisms of early lung specification and branching morphogenesis. Pediatr. Res. 57, 26R–37R.

Weaver, M., Dunn, N.R., Hogan, B.L., 2000. Bmp4 and Fgf10 play opposing roles during lung bud morphogenesis. Development 127, 2695–2704.

Wells, J.M., Melton, D.A., 1999. Vertebrate endoderm development. Annu. Rev. Cell Dev. Biol. 15, 393–410.

Wells, J.M., Melton, D.A., 2000. Early mouse endoderm is patterned by soluble factors from adjacent germ layers. Development 127, 1563–1572.

Williams, M.C., Cao, Y., Hinds, A., Rishi, A.K., Wetterwald, A., 1996. T1 alpha protein is developmentally regulated and expressed by alveolar type I cells, choroid plexus, and ciliary epithelia of adult rats. Am. J. Respir. Cell Mol. Biol. 14, 577–585.

Xu, Q., Wilkinson, D.G., 1998. In situ hybridization: a practical approach. Oxford University Press, London, pp. 87–106.

Yao, J., Lai, E., Stifani, S., 2001. The winged-helix protein brain factor 1 interacts with groucho and hes proteins to repress transcription. Mol. Cell Biol. 21, 1962–1972.

Xu, Y., Farmer, S.R., Smith, B.D., 2007. Peroxisome proliferator-activated receptor gamma interacts with CIITA x RFX5 complex to repress type I collagen gene expression. J. Biol. Chem. 282 (36), 26046–26056.

Yoshida, Y., Kojima, N., Tsuji, S., 1995. Molecular cloning and characterization of a third type of *N*-glycan alpha 2,8-sialyltransferase from mouse lung. J. Biochem. (Tokyo) 118, 658–664.

Zeng, F., Baldwin, D.A., Schultz, R.M., 2004. Transcript profiling during preimplantation mouse development. Dev. Biol. 272, 483–496.